Am J Transl Res 2024;16(6):2645-2653
www.ajtr.org /ISSN:1943-8141/AJTR0155986

Original Article

Quantitative ultrasound imaging parameters in patients with cancerous thyroid nodules: development of a diagnostic model

Mingyang Liu[1], Na Pan[2]

[1]*Department of Ultrasound, Xingtai People's Hospital, No. 16 Hongxing Street, Xingtai 054500, Hebei, China;*
[2]*Department of Hematology, Xingtai People's Hospital, No. 16 Hongxing Street, Xingtai 054500, Hebei, China*

Received February 19, 2024; Accepted April 24, 2024; Epub June 15, 2024; Published June 30, 2024

Abstract: Objective: This study aimed to develop a diagnostic model utilizing quantitative ultrasound parameters to accurately differentiate benign from malignant thyroid nodules. Methods: A retrospective analysis of 194 patients with thyroid nodules, encompassing 65 malignant and 129 benign cases, was performed. Clinical data, ultrasound characteristics, and hemodynamic indicators were compared. Receiver operating characteristic (ROC) curves and logistic regression analysis identified independent diagnostic markers. Results: No significant differences in clinical data were observed between the groups (P>0.05). Malignant nodules, however, were more likely to exhibit solid composition, hypoechoicity, irregular shapes, calcifications, central blood flow, and unclear margins (P<0.05). Hemodynamic parameters showed that malignant nodules had lower end-diastolic volume (EDV) but higher peak systolic velocity (PSV), resistive index (RI), and vascularization flow index (VFI) (P<0.001). Independent diagnostic factors identified included calcification, margin definition, RI, and VFI. A risk prediction model was formulated, demonstrating significantly lower scores for benign nodules (P<0.0001), achieving an ROC area of 0.964. Conclusion: Color Doppler ultrasound effectively distinguishes malignant from benign thyroid nodules. The diagnostic model emphasizes the importance of calcification, margin clarity, RI, and VFI as critical elements, enhancing the accuracy of thyroid nodule characterization and facilitating informed clinical decisions.

Keywords: Color Doppler ultrasound, quantitative imaging parameters, thyroid nodules, diagnostic model, hemodynamics

Introduction

Thyroid cancer is a common malignant tumor of the endocrine system, accounting for approximately 1-2% of all systemic malignant tumors [1]. Recent advances in ultrasound and other imaging technologies have significantly increased the detection rate of thyroid cancer [2], with ultrasound now identifying thyroid nodules in 30-67% of cases, up from a previous 5% [3]. These nodules, often characterized by localized hardness and structural irregularities, are predominantly found in women and increase in prevalence with age [4]. Among individuals evaluated for thyroid nodules, about 7-15% are diagnosed with thyroid cancer, reflecting a global rise in incidence rates of 67% in women and 48% in men over the past three decades [5].

Although most thyroid nodules are benign, a significant number of them evolve into malignant tumors, making thyroid cancer a leading malignancy within the endocrine system [6]. Thyroid cancer includes four primary types: papillary, follicular, medullary, and undifferentiated carcinomas, with papillary carcinoma being the most common and noted for its favorable prognosis and high five-year survival rate [7]. Surgery remains the mainstay of treatment for malignant thyroid nodules, with the primary goal of clinical diagnosis to determine the nodule's nature and tailor the treatment approach accordingly. This strategy helps to avoid unnecessary surgeries and minimize complications, ultimately improving patients' quality of life [8]. However, the subtle onset and diverse nature of thyroid malignancies, along with the overlap in clinical, imaging, and cytological features with

https://doi.org/10.62347/WEDG9279

benign conditions, lead to a significant rate of diagnostic errors in preoperative assessments. These challenges complicate the accurate diagnosis and treatment of benign and malignant thyroid nodules [9].

Imaging techniques, particularly color Doppler ultrasound, are crucial in diagnosing and assessing thyroid nodules [10]. They provide detailed information about the nodule's location, shape, size, texture, and presence of calcifications, facilitating precise evaluation of the nodule's nature and malignancy risk [11]. Color Doppler ultrasound excels in depicting the blood flow distribution within and surrounding the nodule, with malignant nodules typically showing increased blood flow signals [12]. Additionally, quantitative methods such as elastography and acoustic spectroscopy greatly improve the accuracy in differentiating benign from malignant nodules [13]. Hemodynamic parameters, which reflect the speed and direction of blood flow, are vital in assessing the vascular supply to malignant nodules [14]. Nevertheless, the efficacy of color ultrasound in distinguishing benign from malignant nodules requires further investigation and enhancement. Current research is exploring the integration of various imaging techniques with artificial intelligence and machine learning algorithms to enhance diagnostic accuracy and personalize treatment plans, paving the way for future improvements in the diagnostic precision of thyroid nodules and patient outcomes [14].

Building on this foundation, our study aims to thoroughly investigate the expression of quantitative ultrasound imaging parameters in patients with cancerous thyroid nodules and develop a diagnostic model based on these parameters. By analyzing these quantitative ultrasound parameters, we anticipate more accurate distinguishment between benign and malignant thyroid nodules, thus providing a more reliable diagnostic foundation for clinical practice.

Materials and methods

Ethical statement

This study was conducted with the approval of the Medical Ethics Committee of Xingtai People's Hospital, ethical approval number 2022-25A.

Sample sources

The study retrospectively analyzed the data of 254 patients examined at Xingtai People's Hospital from October 10, 2022, to October 9, 2023.

Clinical data collection

Clinical and imaging data were retrieved from the electronic medical record system and during office visits. This included age, sex, disease duration, body mass index, and history of hypertension, diabetes mellitus, smoking, and alcohol abuse. Imaging data comprised texture, internal echogenicity, calcification, morphology, blood flow, margins, end-diastolic volume (EDV), peak systolic velocity (PSV), resistive index (RI), and vascular flow index (VFI).

Diagnostic criteria for benign and malignant nodules

Fine-needle aspiration (FNA) pathology results were classified according to the Bethesda System for Reporting Thyroid Cytopathology [15]. The Bethesda system categorizes findings into six levels: Bethesda Category I: Nondiagnostic or unsatisfactory specimen, unspecified risk of malignancy. Bethesda Category II: Benign nodule, 0-3% risk of malignancy. Bethesda Category III: Atypical or follicular lesion of uncertain significance, 5-15% risk of malignancy. Bethesda Category IV: Follicular neoplasm or follicular tumor suggestive of possible malignancy, 15-30% risk. Bethesda Category V: Suspicious for malignancy, 60-75% risk. Bethesda Category VI: Confirmed malignancy, 97-99% risk.

For this study, nodules classified under Bethesda Categories I and III were excluded due to their inconclusive nature, which often necessitates repeat aspiration. Only nodules classified as Bethesda Category II or confirmed as benign by postoperative pathology were considered benign, while nodules diagnosed as malignant by postoperative pathology were categorized as malignant.

Inclusion exclusion criteria

Inclusion criteria: Patients were eligible for inclusion based on the "Guidelines for the Diagnosis and Treatment of Thyroid Nodules and Differentiated Thyroid Tumors" [16]: 1.

Patients clinically diagnosed with thyroid nodules. 2. Patients who had not received any prior treatment before enrollment. 3. Patients with complete clinical data. 4. Patients who had undergone a surgical pathological diagnosis.

Exclusion criteria: Patients with: 1. Other endocrine system diseases. 2. Severe diffuse lesions of the thyroid gland. 3. A history of neck surgery. 4. Concurrent tumors of other types.

Sample screening and grouping

Out of 254 screened patients, 194 met the eligibility criteria. Based on the diagnostic results, 65 patients with malignant nodules were categorized into the malignant group, and 129 with benign nodules were placed in the benign group.

Observation indicators

Clinical data, ultrasound characteristics, and hemodynamic parameters were compared between the benign and malignant groups. Logistic regression was utilized to identify independent diagnostic indicators, and a diagnostic model was constructed based on the regression beta coefficients.

Statistical analysis

Data analysis was conducted using SPSS software version 26.0, and data visualization was facilitated by GraphPad Prism version 9.00. Measurement data were presented as mean ± standard deviation (mean ± sd), and the t-test was employed for comparisons between the two groups. Count data were presented as cases (%) and analyzed using the chi-squared test. Receiver operating characteristic (ROC) curves were used to determine optimal cut-offs for measured parameters and to evaluate the diagnostic models' effectiveness. Logistic regression was used to analyze independent diagnostic factors. A p-value <0.05 was considered statistically significant.

Results

Comparison of baseline data

An analysis of the baseline clinical data revealed no statistically significant differences between the malignant and benign groups (P>0.05, **Table 1**).

Comparison of ultrasonographic characteristics

The ultrasound imaging characteristics differed significantly between the groups. The malignant group exhibited higher frequencies of solid texture, internal hypoechoicity, calcification, irregular morphology, central blood flow, and unclear margins compared to the benign group, with these differences being statistically significant (P<0.001, **Table 2**).

Comparison of ultrasound hemodynamic parameters

Ultrasound hemodynamic parameters showed that the end-diastolic volume (EDV) was significantly lower in the malignant group, whereas PSV, RI, and VFI were significantly higher compared to the benign group (P<0.001, **Table 3**).

Determination of optimal cut-off values for hemodynamic parameters

For logistic regression analysis, dichotomous categorization of blood flow parameters was based on ROC curve cut-offs. The areas under the curve for EDV, PSV, RI, and VFI were 0.793, 0.703, 0.938, and 0.923 respectively, indicating significant diagnostic potential (**Table 4**; **Figure 1**).

Construction of a diagnostic model for benign and malignant nodules

To develop a diagnostic model for differentiating benign from malignant nodules, we employed multifactorial logistic regression analysis. This analysis identified calcification, rim RI, and VFI as independent diagnostic factors (**Figure 2A**, P<0.05). The diagnostic model was formulated using the β coefficients of these factors, yielding the formula: 'Diagnostic Score = 2.548 × calcification + 1.861 × rim + 4.304 × RI + 3.897 × VFI'. Patients in the malignant nodule group exhibited significantly higher diagnostic scores than those in the benign group (**Figure 2B**, P<0.0001). The ROC curve for this model showed an area under the curve of 0.964 (**Figure 2C**), indicating excellent clinical utility of the model.

Case examples

Sonograms provided illustrate contrasting features between benign and malignant thyroid

Table 1. Comparison of baseline data

Considerations	Malignant group (n = 65)	Benign group (n = 129)	χ^2/value	*P*-value
Age				
≥45 years	36	62	0.927	0.336
<45 years	29	67		
Gender				
Male	29	52	0.329	0.566
Female	36	77		
Course of disease				
≥1 year	42	70	1.898	0.168
<1 year	23	59		
Body mass index				
≥25 kg/m^2	13	19	0.872	0.350
<25 kg/m^2	52	110		
History of hypertension				
Positive	12	19	0.449	0.503
Negative	53	110		
History of diabetes				
Positive	13	19	0.872	0.350
Negative	52	110		
Smoking history				
Positive	33	58	0.585	0.444
Negative	32	71		
History of alcohol abuse				
Positive	7	19	0.584	0.444
Negative	58	110		

Table 2. Comparison of ultrasound characteristics

Considerations	Malignant group (n = 65)	Benign group (n = 129)	χ^2/value	*P*-value
Texture				
Cystic	7	45	13.160	<0.001
Materiality	59	84		
Internal Echo				
Non-echoic	1	10		
High echo	4	38	19.122	<0.001
Low echo	57	78		
Shallow echo	3	3		
Calcification				
Positive	45	20	56.000	<0.001
Negative	20	109		
Morphological				
Rules and Regulations	12	78	30.662	<0.001
Irregularly	53	51		
Blood flow				
Peripheral	16	90	35.553	<0.001
Central	49	39		
Margins				
Clearer	21	108	51.280	<0.001
Unclear	44	21		

Table 3. Comparison of ultrasound hemodynamic parameters

Considerations	Malignant group (n = 65)	Benign group (n = 129)	t-value	*P*-value
EDV (cm/s)	14.18±3.30	18.29±3.90	7.270	<0.001
PSV (cm/s)	34.62±5.87	30.39±4.89	5.311	<0.001
RI	0.77±0.16	0.47±0.10	16.161	<0.001
VFI	4.87±1.42	2.29±0.94	15.037	<0.001

Note: EDV, end-diastolic volume; PSV, peak systolic velocity; RI, resistive index; VFI, vascular flow index.

Table 4. Hemodynamic index ROC parameters

Predictor variable	The area under the curve	95% CI	Sensitivity	Specificity	Cut-off value	Jordon index (math.)
EDV (cm/s)	0.793	0.728-0.858	65.89%	75.39%	16.5	41.28%
PSV (cm/s)	0.703	0.623-0.783	86.82%	46.15%	35.5	32.98%
RI	0.938	0.899-0.977	93.02%	84.62%	0.605	77.64%
VFI	0.923	0.875-0.971	91.47%	84.62%	3.51	76.09%

Note: ROC, receiver operating characteristic; EDV, end-diastolic volume; PSV, peak systolic velocity; RI, resistive index; VFI, vascular flow index.

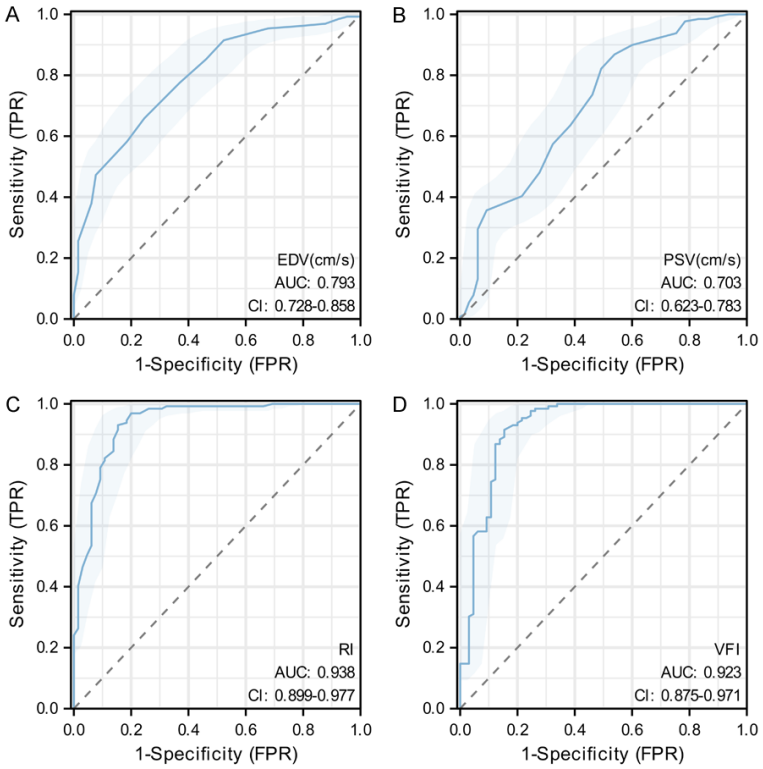

Figure 1. ROC curves of hemodynamic parameters for discriminating between benign and malignant nodule. A. ROC curves for EDV in differentiating benign from malignant nodules. B. ROC curve for PSV in the identification of benign and malignant nodules. C. ROC curve for RI in distinguishing between benign and malignant nodules. D. ROC curve for VFI in the differentiation of benign from malignant nodules. Note: ROC, receiver operating curve; EDV, end-diastolic volume; PSV, peak systolic velocity; RI, resistive index; VFI, vascular flow index; AUC, area under the curve.

nodules. One case, representing a benign lesion, displayed regular margins, homogeneous internal echoes, and effective acoustic transmission, typical of benign nodules. Color Doppler imaging revealed regular blood flow (**Figure 3A**). Conversely, the malignant lesion case showed irregular margins, heterogeneous internal echoes, and potential acoustic shadowing, characteristics often associated with malignancy. Color Doppler imaging in this case indicated abnormal or enhanced blood flow signals (**Figure 3B**), aligning with typical malignant features.

Discussion

Ultrasonography, favored for its noninvasive and radiation-free nature, has become indispensable in diagnosing thyroid diseases. It utilizes both conventional gray-scale and color Doppler ultrasound to provide essential morphological and hemodynamic insights into thyroid nodules, forming a foundational element of the diagnostic process [17]. Research has identified features such as irregular shapes, unclear margins, decreased internal echogenicity, and microcalcifications as key indicators of

A

Factors	β	standard error	Wald	P	Hazard Ratio(95%CI)
Texture	2.136	1.106	3.73	0.053	8.465(0.969-73.964)
Internal Echo	-0.331	1.032	0.103	0.748	0.718(0.095-5.427)
Calcification	2.548	0.871	8.552	0.003	12.782(2.317-70.512)
Morphology	0.476	0.958	0.247	0.619	1.61(0.246-10.519)
blood flow	-0.305	1.396	0.048	0.827	0.737(0.048-11.369)
Boundary	1.861	0.821	5.138	0.023	6.429(1.286-32.129)
EDV	1.647	0.914	3.246	0.072	5.193(0.865-31.166)
PSV	0.012	0.969	<0.001	0.99	1.012(0.152-6.754)
RI	4.304	1.058	16.561	<0.001	73.974(9.309-587.841)
VFI	3.897	0.929	17.586	<0.001	49.232(7.968-304.21)

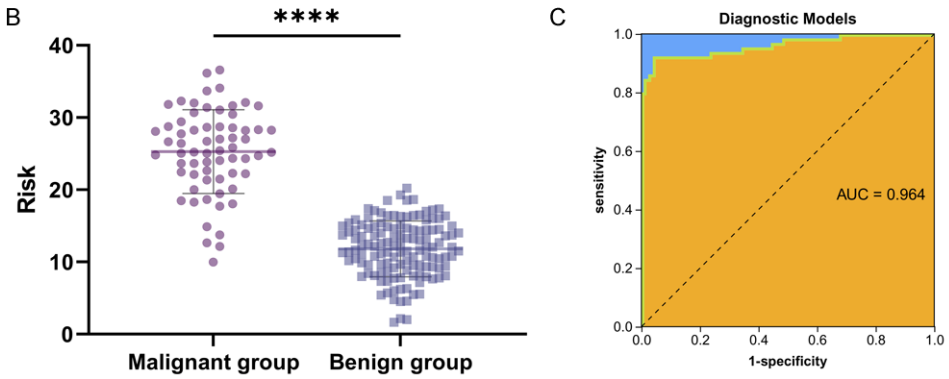

Figure 2. Construction of a diagnostic model for benign and malignant nodules using multifactorial logistic regression. A. Forest plot showing logistic regression of independent diagnostic factors. B. Comparison of diagnostic model scores between malignant and benign nodules. C. The ROC curve of the diagnostic model in predicting benign and malignant nodules. Note: ****P<0.0001 for each. AUC, area under the curve.

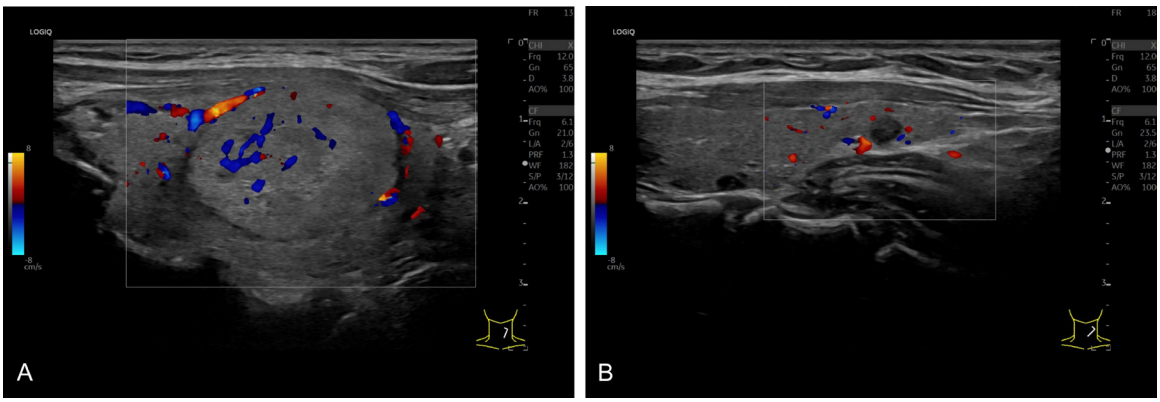

Figure 3. Cases of patients with benign and malignant lesions. A. Benign lesions. B. Malignant lesions.

malignancy [18]. Color Doppler ultrasound, by assessing the vascular patterns within and surrounding the nodules, plays a crucial role in determining their nature. However, the effec-

tiveness of color Doppler in distinguishing benign from malignant nodules is still a subject to debate. Some studies [6] suggest that combining features like microcalcifications, absence of a peripheral halo, and specific blood flow patterns can accurately classify nodules. In contrast, others contend that color Doppler's ability to delineate between benign and malignant nodules is limited due to its focus on smaller blood vessels rather than the microvascular level, potentially missing comprehensive details of the nodules' vascular supply [19]. Additionally, variations in thyroid function, especially in autoimmune thyroid disorders, can obscure vascular signals in thyroid nodules, complicating the assessment of their vascular supply.

Diagnostic models are mathematical or statistical constructs developed by analyzing medical data to predict or ascertain the presence, progression, or outcome of diseases [20, 21]. These models typically rely on indicators such as clinical symptoms, biochemical markers, and imaging features. They utilize algorithms like logistic regression, machine learning, or deep learning to enhance diagnostic accuracy and efficiency, thereby reducing the risk of misdiagnosis and omission. The goal of diagnostic modeling is to provide a more scientific, objective, and quantitative basis for clinical decision-making.

Diagnostic models have become fundamental tools across various medical fields, including cardiovascular disease [22], cancer [23], diabetes [24], and more. These models enable rapid and precise disease diagnosis, support individualized risk assessments, and guide treatment decisions, epitomizing the goals of precision medicine. In the context of thyroid nodule diagnosis, these models evaluate ultrasound features, hemodynamic parameters, and cytopathological findings to determine the benign or malignant nature of nodules, providing essential information for clinical decision-making [25]. Our study identified four independent diagnostic indicators - calcification, unclear margins, RI≥0.605, and VFI≥3.51 - using logistic regression analysis. Calcification, often associated with malignancy, signifies the presence of significant microcalcifications within malignant nodules.

Unclear margins, indicative of the invasive growth of malignant cells, disrupt the architecture of surrounding healthy tissue. Wang et al. [26] confirmed the diagnostic value of calcification and unclear margins, emphasizing their strong correlation with malignancy. RI, measuring vascular resistance, tends to be higher in malignant nodules due to irregular and constricted vascular structures. VFI, which quantifies the volume of blood flow within a nodule, is generally higher in malignant nodules because of their increased vascular supply. These insights corroborate findings by Bakhshaee et al. [27], who noted significant differences in RI, pulsatility index values, and blood flow patterns between benign and malignant nodules in a cohort prepared for thyroid surgery.

These four parameters - calcification, margins clarity, RI, and VFI - offer critical insights for quantitatively distinguishing between benign and malignant thyroid nodules. Utilizing a logistic regression model, we developed a diagnostic tool that not only enhances clinical diagnosis but also underscores the importance and independence of these parameters within the model. Our research resulted in a diagnostic model where scores for patients with malignant nodules were significantly higher than those for patients with benign nodules. The model's ROC curve area was 0.964, demonstrating substantial clinical utility and outperforming the AI model by Ha et al. [28], which recorded an ROC area of 0.939. This indicates that our model may provide greater diagnostic value. Additionally, the nomogram developed by Yi et al. [29] showed an ROC area of 0.936 in the training set and 0.902 in the validation set, further validating our model's superior accuracy and effectiveness. Despite methodological differences between our model and those of Ha et al. [28] and Yi et al. [29], all studies highlight the critical clinical value of advanced diagnostic tools for evaluating thyroid nodules. These models enhance diagnostic precision, offering clinicians rapid, reliable tools for more informed decision-making and optimizing patient treatment strategies.

This study, which employed a logistic regression model, optimized the diagnostic accuracy of thyroid nodules but also identified several limitations. There is a need to increase the amount and diversity of data to enhance the

accuracy and generalizability of the model. Future research could explore various machine learning or deep learning algorithms, possibly in conjunction with other imaging modalities, to further improve diagnostic capabilities. Additionally, integrating parameters related to thyroid function and associated autoimmune diseases may optimize the model. Critical steps for practical implementation include clinical validation, assessment of user acceptance, and thorough training. It is also vital to continuously monitor and evaluate the long-term impact and optimization of these models to ensure they remain effective in supporting clinical diagnosis and patient management.

In conclusion, color Doppler ultrasound effectively reflects the morphology and hemodynamic changes in malignant thyroid nodules. Calcification, margin definition, RI, and VFI are crucial indices for differentiating benign from malignant nodules. The diagnostic model based on these parameters significantly enhances the accuracy of identifying the nature of thyroid nodules and provides a vital reference for clinical treatment decisions.

Disclosure of conflict of interest

None.

Address correspondence to: Mingyang Liu, Department of Ultrasound, Xingtai People's Hospital, No. 16 Hongxing Street, Xingtai 054500, Hebei, China. E-mail: lmyhnd@126.com

References

[1] Haddad RI, Bischoff L, Ball D, Bernet V, Blomain E, Busaidy NL, Campbell M, Dickson P, Duh QY, Ehya H, Goldner WS, Guo T, Haymart M, Holt S, Hunt JP, Iagaru A, Kandeel F, Lamonica DM, Mandel S, Markovina S, McIver B, Raeburn CD, Rezaee R, Ridge JA, Roth MY, Scheri RP, Shah JP, Sipos JA, Sippel R, Sturgeon C, Wang TN, Wirth LJ, Wong RJ, Yeh M, Cassara CJ and Darlow S. Thyroid carcinoma, version 2.2022, NCCN clinical practice guidelines in oncology. J Natl Compr Canc Netw 2022; 20: 925-951.

[2] Crockett DJ, Faucett EA and Gnagi SH. Thyroid nodule/differentiated thyroid carcinoma in the pediatric population. Pediatr Ann 2021; 50: e282-e285.

[3] Alexander LF, Patel NJ, Caserta MP and Robbin ML. Thyroid ultrasound: diffuse and nodular disease. Radiol Clin North Am 2020; 58: 1041-1057.

[4] Jiang L, Zhang D, Chen YN, Yu XJ, Pan MF and Lian L. The value of conventional ultrasound combined with superb microvascular imaging and color Doppler flow imaging in the diagnosis of thyroid malignant nodules: a systematic review and meta-analysis. Front Endocrinol (Lausanne) 2023; 14: 1182259.

[5] Abbasian Ardakani A, Bitarafan-Rajabi A, Mohammadi A, Hekmat S, Tahmasebi A, Shiran MB and Mohammadzadeh A. CAD system based on B-mode and color Doppler sonographic features may predict if a thyroid nodule is hot or cold. Eur Radiol 2019; 29: 4258-4265.

[6] Maddaloni E, Briganti SI, Crescenzi A, Beretta Anguissola G, Perrella E, Taffon C, Palermo A, Manfrini S, Pozzilli P and Lauria Pantano A. Usefulness of color Doppler ultrasonography in the risk stratification of thyroid nodules. Eur Thyroid J 2021; 10: 339-344.

[7] Wang M, Wang X and Zhang H. Grayscale, subjective color Doppler, combined grayscale with subjective color Doppler in predicting thyroid carcinoma: a retrospective analysis. Braz J Otorhinolaryngol 2022; 88: 220-227.

[8] Song D, Dong F, Zheng J, Luo H and Wei J. Application value of color Doppler ultrasonography combined with thyroid autoantibody tests in early diagnosis of thyroid cancer. Comput Math Methods Med 2022; 2022: 5248230.

[9] Blum M. Ultrasonography of the thyroid. In: Feingold KR, Anawalt B, Blackman MR, Boyce A, Chrousos G, Corpas E, de Herder WW, Dhatariya K, Dungan K, Hofland J, Kalra S, Kaltsas G, Kapoor N, Koch C, Kopp P, Korbonits M, Kovacs CS, Kuohung W, Laferrère B, Levy M, McGee EA, McLachlan R, New M, Purnell J, Sahay R, Shah AS, Singer F, Sperling MA, Stratakis CA, Trence DL, Wilson DP, editors. Endotext. South Dartmouth (MA): MDText.com, Inc. Copyright © 2000-2023, MDText.com, Inc.; 2000.

[10] Darvish L, Khezri M, Teshnizi SH, Roozbeh N, Dehkordi JG and Amraee A. Color Doppler ultrasonography diagnostic value in detection of malignant nodules in cysts with pathologically proven thyroid malignancy: a systematic review and meta-analysis. Clin Transl Oncol 2019; 21: 1712-1729.

[11] Li HJ, Yang YP, Liang X, Zhang Z and Xu XH. Comparison of the diagnostic performance of three ultrasound thyroid nodule risk stratification systems for follicular thyroid neoplasm: K-TIRADS, ACR-TIRADS and C-TIRADS. Clin Hemorheol Microcirc 2023; 85: 395-406.

[12] Zhu YC, Zhang Y, Deng SH and Jiang Q. A prospective study to compare superb microvascular imaging with grayscale ultrasound and col-

or Doppler flow imaging of vascular distribution and morphology in thyroid nodules. Med Sci Monit 2018; 24: 9223-9231.
[13] Karagülle M, Arslan FZ, Şimşek S, Öncü S, Pamuk GG, Öncü M and Tan Cimilli A. Investigation of the effectiveness of microvascular Doppler ultrasound and Q-Pack in the discrimination of malign thyroid nodules from benign. Ultrasound Q 2023; 39: 37-46.
[14] Akkus Z, Cai J, Boonrod A, Zeinoddini A, Weston AD, Philbrick KA and Erickson BJ. A survey of deep-learning applications in ultrasound: artificial intelligence-powered ultrasound for improving clinical workflow. J Am Coll Radiol 2019; 16: 1318-1328.
[15] Trimboli P, Scappaticcio L, Treglia G, Guidobaldi L, Bongiovanni M and Giovanella L. Testing for BRAF (V600E) mutation in thyroid nodules with fine-needle aspiration (FNA) read as suspicious for malignancy (Bethesda V, Thy4, TIR4): a systematic review and meta-analysis. Endocr Pathol 2020; 31: 57-66.
[16] Lee JY, Baek JH, Ha EJ, Sung JY, Shin JH, Kim JH, Lee MK, Jung SL, Lee YH, Ahn HS, Yoon JH, Choi YJ, Park JS, Lee YJ, Choi M and Na DG; Korean Society of Thyroid Radiology (KSThR) and Korean Society of Radiology. 2020 imaging guidelines for thyroid nodules and differentiated thyroid cancer: Korean Society of Thyroid Radiology. Korean J Radiol 2021; 22: 840-860.
[17] Schmidt D. Ultrasound of thyroid nodules - ultrasound characteristics and risk of carcinoma. Laryngorhinootologie 2019; 98: 79-84.
[18] Saade-Lemus SM, Sridharan A, Smitthimedhin A, Bauer A, Cahill AM, Darge K and Hwang M. Advanced ultrasound techniques for differentiation of benign versus malignant thyroid nodules: a review. Ultrasound Q 2021; 37: 315-323.
[19] Xue N, Li P, Deng H, Yi J, Xie Y and Zhang S. The spoke wheel color Doppler blood flow signal is a specific sign of papillary thyroid carcinoma. Front Endocrinol (Lausanne) 2022; 13: 1030143.
[20] Myers J, Kei J, Aithal S, Aithal V, Driscoll C, Khan A, Manuel A, Joseph A and Malicka AN. Development of a diagnostic prediction model for conductive conditions in neonates using wideband acoustic immittance. Ear Hear 2018; 39: 1116-1135.
[21] Frondelius T, Atkova I, Miettunen J, Rello J and Jansson MM. Diagnostic and prognostic prediction models in ventilator-associated pneumonia: systematic review and meta-analysis of prediction modelling studies. J Crit Care 2022; 67: 44-56.
[22] Liu K, Chen S and Lu R. Identification of important genes related to ferroptosis and hypoxia in acute myocardial infarction based on WGCNA. Bioengineered 2021; 12: 7950-7963.
[23] Yamashita R, Long J, Longacre T, Peng L, Berry G, Martin B, Higgins J, Rubin DL and Shen J. Deep learning model for the prediction of microsatellite instability in colorectal cancer: a diagnostic study. Lancet Oncol 2021; 22: 132-141.
[24] Wu B, Niu Z and Hu F. Study on risk factors of peripheral neuropathy in type 2 diabetes mellitus and establishment of prediction model. Diabetes Metab J 2021; 45: 526-538.
[25] Xu H, Zhang Y, Wu H, Zhou N, Li X, Pineda JP, Zhu Y, Fu H, Ying M, Yang S, Bao J, Yang L, Zhang B, Guo L, Sun L, Lu F, Wang H, Huang Y, Zhu T, Wang X, Wei Q, Sheng C, Qu S, Lv Z, Xu D, Li Q, Dong Y, Qin J, Cheng T and Xing M. High diagnostic accuracy of epigenetic imprinting biomarkers in thyroid nodules. J Clin Oncol 2023; 41: 1296-1306.
[26] Wang ZF, Shang J, Zhu Y and Liu B. Role of contrast-enhanced ultrasound in distinguishing between benign and malignant thyroid nodules with calcification. Zhongguo Yi Xue Ke Xue Yuan Xue Bao 2021; 43: 905-910.
[27] Bakhshaee M, Davoudi Y, Mehrabi M, Layegh P, Mirsadaee S, Rad MP and Leyegh P. Vascular pattern and spectral parameters of power Doppler ultrasound as predictors of malignancy risk in thyroid nodules. Laryngoscope 2008; 118: 2182-2186.
[28] Ha EJ, Lee JH, Lee DH, Moon J, Lee H, Kim YN, Kim M, Na DG and Kim JH. Artificial intelligence model assisting thyroid nodule diagnosis and management: a multicenter diagnostic study. J Clin Endocrinol Metab 2024; 109: 527-535.
[29] Yi D, Fan L, Zhu J, Yao J, Peng C and Xu D. The diagnostic value of a nomogram based on multimodal ultrasonography for thyroid-nodule differentiation: a multicenter study. Front Oncol 2022; 12: 970758.